

Three-dimensional simulations of a starburst wind

Jackie L. Cooper · Geoffrey V. Bicknell ·
Ralph S. Sutherland · Joss Bland-Hawthorn

Received: 4 March 2007 / Accepted: 9 May 2007 / Published online: 5 June 2007
© Springer Science+Business Media B.V. 2007

Abstract In order to better understand the formation of a starburst-driven wind, we have performed a series of three-dimensional hydrodynamical simulations in an inhomogeneous interstellar medium. We present the results of these simulations, which provide new insights into the formation of the optical filaments and the origin of the soft X-ray emission.

Keywords Galaxies: starburst · Hydrodynamics · ISM: jets & outflows · Method: numerical

1 Introduction

Galactic winds are ubiquitous in starburst galaxies, having been observed in all nearby starburst galaxies and inferred in galaxies at high redshifts (Veilleux et al. 2005). A starburst is able to power a galactic-scale wind due to its characteristically high star formation rate, the main product of which are large OB stars. The energy from the stellar winds and supernovae produced by these stars drives an outflow-

ing of gas along the minor axis of the galaxy (Chevalier and Clegg 1985). Observations of these winds at optical wavelengths (e.g. H α) reveal vast (\sim few kpc) filamentary structures extending along the minor axis of the galaxy. These filaments display varying morphologies, and are known to be both limb-brightened (e.g. M82: Shopbell and Bland-Hawthorn 1998) and distributed throughout the wind (e.g. Circinus: Veilleux and Bland-Hawthorn 1997). At X-ray wavelengths, recent Chandra observations have revealed increasing structure in the soft X-ray emission. In particular, a spatial correlation between the soft X-ray and filamentary H α emission is now known to exist (e.g. Cecil et al. 2002; Strickland et al. 2004). This is suggestive of a physical relationship, which is still not well understood.

While starburst winds have been modeled in the past (e.g. Tomisaka and Bregman 1993; Suchkov et al. 1994; Strickland and Stevens 2000), these models were axisymmetric. Additionally, the interstellar medium in each model is necessarily homogeneous. While these simulations provide useful insights into the structure and formation of a galactic wind, the constraint of axisymmetry limits their ability to form significant filamentary structures and consequently constrain the related soft X-ray emission.

In order to improve upon these prior simulations, we have performed a series of three-dimensional simulations of a starburst wind in an inhomogeneous interstellar medium designed to test the effect of the interstellar medium on the resulting outflow. We have investigated the mechanism behind the formation of the emission line filaments and we also propose an origin for the soft X-ray emission.

2 Numerical method

The simulations were performed using a Piecewise Parabolic Method with a Lagrangian Remap (PPMLR) based

J.L. Cooper (✉) · G.V. Bicknell · R.S. Sutherland
Research School of Astronomy and Astrophysics, Australian
National University, Mt Stromlo Observatory, Cotter Rd,
Weston Creek, ACT 2611, Australia
e-mail: jcooper@mso.anu.edu.au

G.V. Bicknell
e-mail: geoff@mso.anu.edu.au

R.S. Sutherland
e-mail: ralph@mso.anu.edu.au

J. Bland-Hawthorn
Anglo-Australian Observatory, PO Box 296, Epping, NSW 2121,
Australia
e-mail: jbh@aoa.gov.au

on the method described by Colella and Woodward (1984). Thermal cooling and more sophisticated shock algorithms were added to the code, which was also optimised for use on the Australian Partnership for Advanced Computation (APAC) Altix computer. The resolution of each three-dimensional simulation is $512 \times 512 \times 512$ cells, covering a spatial range of 1 kpc³.

Following Strickland and Stevens (2000), the simulations incorporate a two component gravitational potential, consisting of a stellar spheroid described by an analytic King model and a Miyamoto and Nagai (1975) disk potential. The ISM consists of a hot uniform halo and a warm inhomogeneous disk, which are in pressure equilibrium with $P/k = 10^6$ cm⁻³ K. The hot halo is static, with temperature $T_h = 5 \times 10^6$ K and density $\rho_h = 0.2$ cm⁻³. The warm inhomogeneous disk is rotating and has an average temperature of $T_d = 10^4$ K and mean density:

$$\frac{\bar{\rho}_{\text{disk}}(r, z)}{\bar{\rho}_{\text{disk}}(0, 0)} = \exp \left[-\frac{\Phi_{\text{tot}}(r, z) - e_d^2 \Phi_{\text{tot}}(r, 0) - (1 - e_d^2) \Phi_{\text{tot}}(0, 0)}{\sigma_t^2 + c_{s,d}^2} \right] \quad (1)$$

where $c_{s,d} = \sqrt{k T_d / \mu m}$ is the mean sound speed of the warm gas, σ_t is the turbulent velocity dispersion of the clouds, and

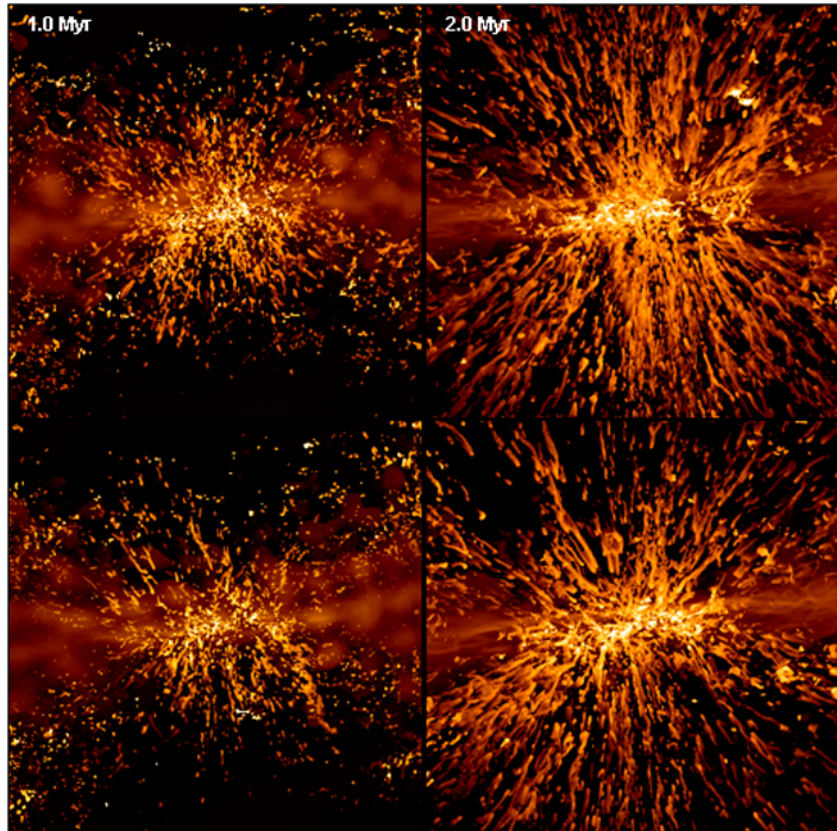
Fig. 1 Filamentary H α emission at 1 Myr (left) and 2 Myr (right) epochs. The upper and lower panels represent two different models that vary only by the distribution of clouds in the disk

e_d is the ratio of the azimuthal to the Keplerian velocity of the warm gas (see Sutherland and Bicknell 2007).

To power an outflow, we define a cylindrical starburst region of radius $r_{\text{sb}} = 150$ pc and height $h_{\text{sb}} = 60$ pc, positioned on the center of the computational grid. Mass and energy is injected into this region proportional to the density, at a rate of $\dot{M} = 1 M_\odot \text{ yr}^{-1}$ and $\dot{E} = 10^{42} \text{ erg s}^{-1}$ respectively, continuously over the course of each simulation.

3 Filamentary H α emission

Perhaps the most spectacular feature of a starburst wind are the filaments seen at optical wavelengths (e.g. H α , N II). These filaments display varying morphologies, ranging from the biconical outflow in M82 (Shopbell and Bland-Hawthorn 1998), to the bubble shaped wind in NGC 3079 (Veilleux et al. 1994). Figure 1 shows the simulated H α emission in two models, which vary only by the initial distribution of clouds in the disk. The H α emitting material is defined to be disk gas that has a temperature in the range of $5 \times 10^3 - 3 \times 10^4$ K. The filaments appear as strings of clouds that emanate from the starburst region and rotate in the same direction as the disk. In both models, the filaments have velocities of $v \sim 100-800 \text{ km s}^{-1}$, similar to those observed in M82 (Shopbell and Bland-Hawthorn 1998; Greve 2004).



The mechanism behind the formation of the filaments in our simulations is as follows: energy is injected into the dense clouds in the starburst region. As the binding energy of the clouds is overcome, they begin to fragment. The fragments are then accelerated into the outflow by the ram pressure of the wind. Filaments are also formed from gas that is stripped from the edge of the starburst region and entrained into the outflow (see Cooper et al. 2007).

The interstellar medium of a galaxy plays an important role in shaping an outflow. The unique cloud distributions in the upper and lower panels of Fig. 1 result in the formation of winds that exhibit differing morphologies. This is seen at both 1 and 2 Myr epochs, where the distribution of the filaments varies between models. In the first model (upper panels), the filaments form a biconical structure, reminiscent of the outflow in M82 (Shopbell and Bland-Hawthorn 1998). In the second model (lower panels) the filaments are more chaotic, with the biconical structure less defined. It is likely that the location of the clouds in the starburst region influences the morphology of the filament system.

The filaments produced in our simulations are volume filled, in agreement with observations of the wind in the Circinus Galaxy (Veilleux and Bland-Hawthorn 1997). However, many starburst winds, such as M82 (Shopbell and Bland-Hawthorn 1998) and NGC 3079 (Veilleux et al. 1994), are limb-brightened, indicating that the filaments reside on the surface of a mostly hollow structure. Given the mechanism behind the formation of filaments in our simulations, it is likely that a limb-brightened outflow reflects the structure of starburst region. An outflow powered by a torus

shaped starburst region (Telesco et al. 1993) would likely result in filaments that predominantly flow along the walls of an empty biconical structure. An alternative explanation is that a wind powered by an earlier burst of star formation has evacuated the center of the starburst region (e.g. Bland-Hawthorn and Cohen 2003).

As photoionization is not included in our model, the H α filaments are all shock ionized. Indeed, this is the case with the outflow in NGC 1482 (Veilleux and Rupke 2002). On the other hand, many outflows show signs of photoionization, such as the strong ionization cone in M82, where emission in the lower filaments are thought to be due to photoionization, with shocks becoming the dominant mechanism at larger radii (Shopbell and Bland-Hawthorn 1998). Photoionization likely plays an important role in the excitation of filaments in starburst winds.

4 Origin of the soft X-ray emission

The soft (0.5–2.0 kev) X-ray emission arising from our model was determined using broadband cooling fractions obtained from MAPPINGS IIIr (see Sutherland and Dopita 1993). Figure 2 shows the soft X-ray emissivity through the central y plane of one of our models at 1 Myr (left) and 2 Myr (right) epochs. At 1 Myr the structure of the wind resembles that of a wind-blown superbubble in the “snowplow” phase of its evolution (see Tomisaka and Ikeuchi 1988). The main X-ray feature is the swept-up shell of halo gas, which has been shock heated to temperatures of $T \sim 7 \times 10^6$ K.

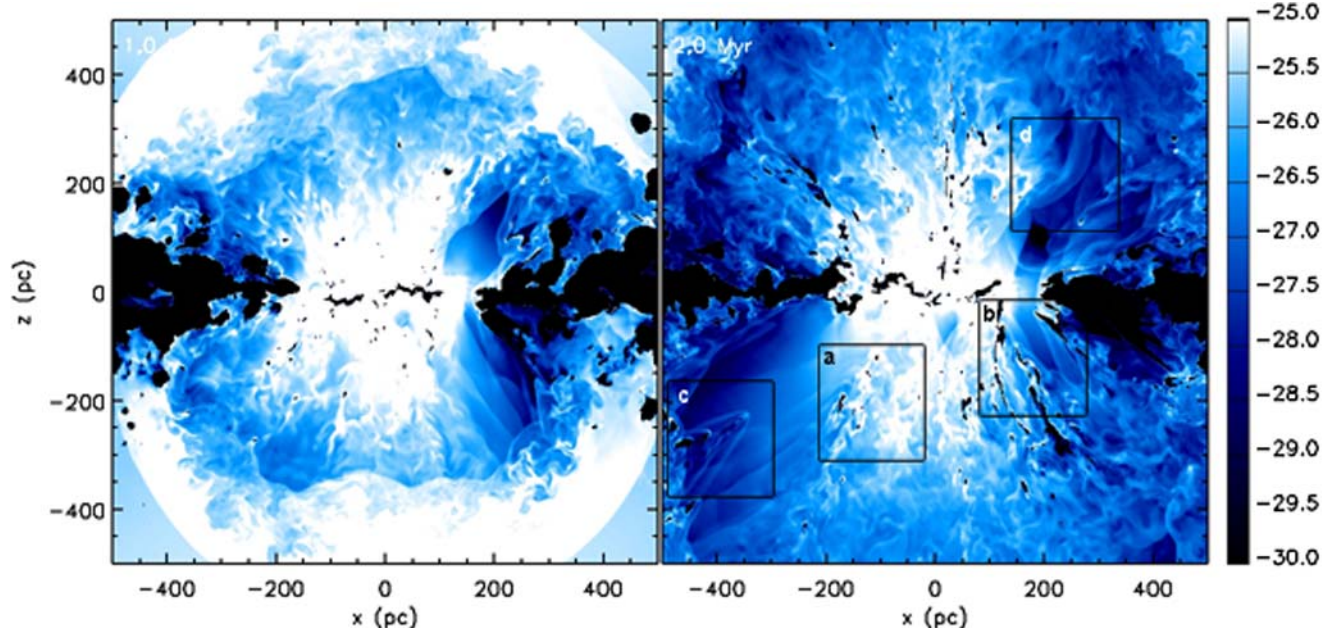


Fig. 2 Logarithm of the soft X-ray emissivity ($\text{erg s}^{-1} \text{cm}^{-3}$) through the $y = 0$ plane at 1 Myr (left) and 2 Myr (right) epochs. The boxes in the right-hand panel indicate regions of soft X-ray emission highlighted in Fig. 3

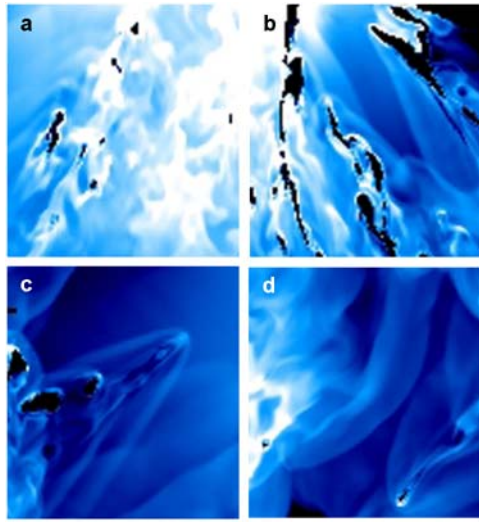


Fig. 3 Highlighted soft X-ray emissivity: (a) the cooling mass-loaded wind, (b) the intermediate temperature interface between the hot and cold gas, (c) bow shocks, and (d) the interaction between bow shocks

At 2 Myr the X-ray emitting shell has flown off the edge of the computational grid and the soft X-ray emission arises solely from four main processes in the “free-wind” region of the outflow. Examples of these processes are shown in Fig. 3:

- The mass-loaded wind. The mixing of hot gas in the vicinity of the starburst region with clouds in the disk results in the production of a hot ($T \gtrsim 10^6$ K), mass-loaded ($n \sim 0.3 \text{ cm}^{-3}$) wind that is rapidly cooling. This strongly emitting X-ray feature is the largest contributor to the soft X-ray emission.
- The intermediate temperature ($T \sim 10^6$ K) interface between the hot wind and the cooler filaments. Soft X-rays arise from a region of intermediate density and temperature that is created due to mixing at the interface.
- Bow shocks. Soft X-rays arise when a bow shock ($T \sim 10^7$ K) forms upstream of clouds of disk gas that have been accelerated into the outflow.
- Colliding bow shocks. As the wind expands, the bow shocks that have formed via process (c) begin to cool. When two shocks interact, the gas is further shock heated to temperatures of the order $T \sim 10^7$ K.

It should be noted that mechanisms (a) and (b) both involve the mixing of high temperature gas from the hot wind and warm gas from the filaments to produce gas of an intermediate temperature that strongly emits soft X-rays. The numerical resolution of these simulations is insufficient to resolve the fine scale interactions of this gas and we can only consider soft X-ray emission arising via mixing to be a possible mechanism at this stage. The interaction of cooling clouds with a wind has been investigated by Mellema et al. (2002) who demonstrated the break-up and survival of

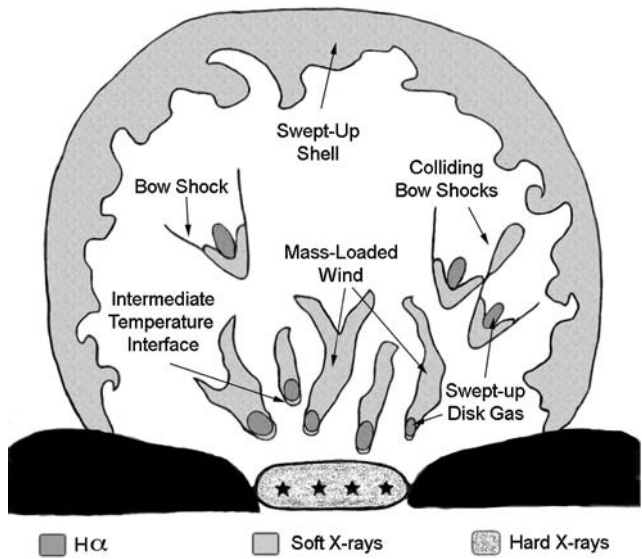


Fig. 4 Schematic of the H α and X-ray emission arising in a starburst wind and their spatial relationship

clouds in a flow. However, their two-dimensional calculations do not adequately address the mixing of hot and cold gas, which is a three-dimensional phenomenon. Higher resolution simulations are planned in order to better address this issue.

By extrapolating from the structure of the outflow at 1 and 2 million years in Fig. 2, we can infer the origin of the soft X-ray emission at later times. Figure 4 shows a schematic of the X-ray and H α emission in a starburst wind, based on the results of our simulations. The mechanism behind the formation of the filaments in our model naturally leads to the production of soft X-rays. Bow shocks emitting at soft X-ray energies form upstream of clouds of disk gas that are accelerated into the outflow. These clouds are also potentially a source of mass-loading, with tails of soft X-ray emitting gas streaming from their surfaces. X-ray emission that arises from the processes listed above provide a natural explanation for the spatial correlation that is now known to exist between the H α and soft X-ray emitting gas. However, the strongly soft X-ray emitting shell of swept-up gas has no associated H α emission. This possibly argues for the presence of soft X-ray emission beyond the extent of the H α emission in a starburst wind, but due to the limited spatial range of these simulations, the ultimate fate of the swept-up shell is not known. As found in previous simulations of starburst-driven winds, it is possible that the shell cools radiatively to below X-ray temperatures or is broken-up by Rayleigh–Taylor instabilities (see, for example, Tomisaka and Bregman 1993).

As was found to be the case with the H α emission, the soft X-ray gas in our model is volume filled. While many winds are known to limb-brightened in X-rays, there is some evidence to suggest that starburst-driven outflows may

at least be partially volume filled (e.g. NGC 3079: Cecil et al. 2002). The same mechanism behind the formation of a limb-brightened outflow in H α would likely result in limb-brightened X-ray emission.

5 Summary

- We have performed a series of three dimensional simulations of a starburst wind in an inhomogeneous interstellar medium. These simulations were designed to test the impact of the ISM on the formation of a wind.
- The morphology of a starburst-driven wind is highly dependent on the structure and nature of the interstellar medium in which it forms.
- Filaments are formed from the breakup of clouds in the starburst region, the fragments of which are then accelerated into the outflow by the ram pressure of the wind. Filaments are also formed from gas stripped from the sides of the starburst region and entrained into the outflow. These filaments form a volume filled biconical structure.
- We find four processes that lead to the production of soft X-rays which would explain the observed spatial correlation between the soft X-ray and H α emitting gas. These processes are: The mass-loaded wind, the intermediate temperature interface between the hot wind and cooler filaments, the interaction between bow shocks, and the bow shocks themselves. As noted earlier, X-ray emission from mixing processes need further investigation in order to determine their significance.

References

- Bland-Hawthorn, J., Cohen, M.: The large-scale bipolar wind in the galactic center. *Astrophys. J.* **582**, 246–256 (2003)
- Cecil, G., Bland-Hawthorn, J., Veilleux, S.: Tightly correlated X-ray/H α -emitting filaments in the superbubble and large-scale superwind of NGC 3079. *Astrophys. J.* **576**, 745–752 (2002)
- Chevalier, R.A., Clegg, A.W.: Wind from a starburst galaxy nucleus. *Nature* **317**, 44 (1985)
- Colella, P., Woodward, P.R.: The piecewise parabolic method (PPM) for gas-dynamical simulations. *J. Comput. Phys.* **54**, 174–201 (1984)
- Cooper, J.L., Bicknell, G.V., Sutherland, R.S., Bland-Hawthorn, J.: Three-dimensional simulations of a starburst-driven galactic wind. *Astrophys. J.* (2007, submitted)
- Greve, A.: The rotating visible outflow in M82. *Astron. Astrophys.* **416**, 67–78 (2004)
- Mellema, G., Kurk, J.D., Röttgering, H.J.A.: Evolution of clouds in radio galaxy cocoons. *Astron. Astrophys.* **395**, L13–L16 (2002).
- Miyamoto, M., Nagai, R.: Three-dimensional models for the distribution of mass in galaxies. *Publ. Astron. Soc. Jpn.* **27**, 533–543 (1975)
- Shopbell, P.L., Bland-Hawthorn, J.: The asymmetric wind in M82. *Astrophys. J.* **493**, 129 (1998)
- Strickland, D.K., Heckman, T.M., Colbert, E.J.M., Hoopes, C.G., Weaver, K.A.: A high spatial resolution X-ray and H α study of hot gas in the Halos of star-forming disk galaxies. I. Spatial and spectral properties of the diffuse X-ray emission. *Astrophys. J. Suppl. Ser.* **151**, 193–236 (2004)
- Strickland, D.K., Stevens, I.R.: Starburst-driven galactic winds – I. En-ergetics and intrinsic X-ray emission. *Mon. Not. Roy. Astron. Soc.* **314**, 511–545 (2000)
- Suchkov, A.A., Balsara, D.S., Heckman, T.M., Leitherer, C.: Dynamics and X-ray emission of a galactic superwind interacting with disk and halo gas. *Astrophys. J.* **430**, 511–532 (1994)
- Sutherland, R.S., Bicknell, G.V.: Interactions of a light hypersonic jet with a non-uniform interstellar medium. *Astrophys. J. Suppl. Ser.* (2007, submitted)
- Sutherland, R.S., Dopita, M.A.: Cooling functions for low-density astrophysical plasmas. *Astrophys. J. Suppl. Ser.* **88**, 253–327 (1993).
- Telesco, C.M., Dressel, L.L., Wolstencroft, R.D.: The genesis of starbursts and infrared emission in the centers of galaxies. *Astrophys. J.* **414**, 120–143 (1993).
- Tomisaka, K., Bregman, J.N.: Extended hot-gas halos around starburst galaxies. *Publ. Astron. Soc. Jpn.* **45**, 513–528 (1993)
- Tomisaka, K., Ikeuchi, S.: Starburst nucleus—Galactic-scale bipolar flow. *Astrophys. J.* **330**, 695–717 (1988)
- Veilleux, S., Bland-Hawthorn, J.: Artillery shells over Circinus. *Astrophys. J. Lett.* **479**, L105 (1997)
- Veilleux, S., Cecil, G., Bland-Hawthorn, J., Tully, R.B., Filippenko, A.V., Sargent, W.L.W.: The nuclear superbubble of NGC 3079. *Astrophys. J.* **433**, 48–64 (1994)
- Veilleux, S., Cecil, G., Bland-Hawthorn, J.: Galactic winds. *Annu. Rev. Astron. Astrophys.* **43**, 769–826 (2005)
- Veilleux, S., Rupke, D.S.: Identification of galactic wind candidates using excitation maps: tunable-filter discovery of a shock-excited wind in the galaxy NGC 1482. *Astrophys. J. Lett.* **565**, L63–L66 (2002).